Rough sea surface scattering with a wide angle Parabolic Equation model and comparison to a simple surface loss method

M. K. Donnelly, R. N. Hewitt

Underwater Sensors and Oceanography department, DERA, Winfrith Technology Centre, Dorset, UK.
rhewitt@dera.gov.uk

Abstract

Underwater acoustic propagation models traditionally treat the sea surface as a flat, horizontal lossy boundary, at which a surface loss formula is applied. This approach reduces the amplitude of surface-interacting acoustic paths according to the chosen reflection loss formula. Whilst this approach may be satisfactory for many applications, it is approximate in that there is no re-distribution of acoustic energy with angle as will occur in reality. The interaction of an acoustic pressure field with a rough boundary is a complex process and the surface loss formula can only attempt to represent its gross effects in an approximate manner. In order to understand the limitations of the surface loss formula approach, results must be compared to those from a full surface scattering implementation. We present a rough sea surface scattering implementation within a wide angle parabolic equation model, and verify our implementation by comparison with results from a numerically precise Helmholtz integral method. A surface loss formula has also been implemented in the same parabolic equation model in order to compare directly surface scattering to surface loss results. We present single frequency results and pulse results obtained via Fourier synthesis. The differences in results from the two methods are discussed.

1. Introduction

The interaction of sound with the sea surface is a complex process, and involves scattering from a moving rough boundary and attenuation and scattering due to bubble clouds. The dominant effects are frequency dependent, with bubble effects becoming more significant at frequencies of several kilohertz. For frequencies of around 1 kHz, the problem is primarily one of rough boundary scattering. Approaches to the surface scattering problem have often focussed on frequencies for which the ratio of acoustic wavelength to surface wavelength or wave height is much greater than or much less than one [1]. In the first case, the scattering effects can be modelled using perturbation methods; in the second case a geometrical ray approach is often used in which the sea surface is considered to be locally planar to an incoming ray of sound and the ray reflected accordingly. These methods are relatively simple to implement, but have limited validity when the acoustic wavelength and surface features are of comparable size, which is a more complicated problem with diffraction as a dominant effect.

Ocean-acoustic propagation models often treat the sea surface as a horizontal flat lossy boundary. Acoustic paths interacting with the surface suffer a frequency-dependent amplitude reduction per surface bounce (this may be angle-dependent), but the boundary is planar and the gross scattering effects are modelled simply as a loss. This approach may be adequate for many problems, but it is a simplistic approach to a complex problem.

DERA have developed the Synthetic Pulse Reception (SPUR) model [2,3] which predicts the propagation of acoustic pulses through ocean environments. SPUR is based upon Fourier Synthesis of single frequency parabolic equation (PE) solutions provided by a modified and enhanced version of the Range-dependent Acoustic Model (RAM) [4]. The effect of the ocean environment upon a pulse is therefore represented by a transfer function, the coefficients of which are obtained from the modified version of RAM. Both single frequency and pulse solutions can be provided for propagation through complex range-dependent ocean environments. The environment consists of a water layer overlying one or more seafloor layers, with an upper halfspace to simulate either surface loss or scattering (discussed below). Each layer can have arbitrary bathymetry and depth-dependent profiles (sound speed, density and attenuation), and the profiles can change with range. Two of the enhancements to RAM are the inclusion of a surface loss formula and a surface scattering method. These alternate treatments of the sea surface allow for comparisons of results from the surface loss and surface scattering methods.

Here the surface loss and surface scattering methods are discussed, and results from the scattering method are validated by comparison to the numerically precise Helmholtz integral method, which provides benchmark

TG Leighton, GJ Heald, HD Griffiths, G Griffiths, (eds.), 'Acoustical Oceanography', Proc. Institute of Acoustics Vol. 23 Part 2, 2001.

solutions. Both single frequency and pulsed results are then computed for a shallow water environment with a reflective seabed. Results produced using both the surface loss and scattering methods are compared.

2. Sea surface representation

2.1 Surface loss formula implementation

The surface loss formula used is based upon experimental data from low angle measurements in a lake and is also consistent with measurements reported by Weston [5].

$$SL = -20\log_{10}\left(0.3 + \frac{0.7}{1+1.92\times10^{-11} f^2 v^4}\right) \tag{1}$$

In (1) SL is the surface reflection loss in dB per bounce, f is frequency in Hz and v is wind speed in ms^{-1}. The surface loss formula is implemented as a half-space overlying the water layer with density selected to give the prescribed surface loss. As the formula is angle-independent, sound speed will be constant across the interface between the water layer and the half-space. The required surface loss is achieved by simple plane-wave reflection loss considerations.

$$\frac{\rho_s - 1}{\rho_s + 1} = 0.3 + \frac{0.7}{1+1.92\times10^{-11} f^2 v^4} \tag{2}$$

In (2) the plane-wave amplitude reflection coefficient has been equated to that prescribed by the surface loss formula. The equation is then solved to find the density used for the upper half-space, ρ_s. The half-space is implemented as a layer with an overlying absorbing layer having the same sound speed and density but with attenuation so as to prevent any false reflections from the environment ceiling (pressure release condition).

2.2 Surface scattering implementation

Depth-discretisation of the ocean environment is handled in RAM by the Galerkin method [6]. The Galerkin method does not require the implementation of interface conditions (continuity of pressure and normal particle displacement velocity) between different environmental layers. Instead, interfaces are modelled by changing the parameters encompassing the sound speed, density and attenuation at the interface depth. An interface is hence modelled as a rapid linear transition between the different environmental layer properties. Implementation of a range-dependent interface is therefore very straightforward: the depths at which the parameters change simply change with range. Our method involves the implementation of an actual sea surface profile, i.e. a sea surface elevation as a function of range, as simply an interface between the water layer and an air upper half-space with the actual environmental properties of air. This is merely another range-dependent interface regardless of its environmental properties. The surface profile can be arbitrary, but the implementation in SPUR is based upon the Pierson-Moskowitz [7] sea surface wave spectrum, which is a well established analytical sea surface wave spectrum for a fully developed sea.

$$A(\chi) = \frac{5.5}{v}\sqrt{\frac{6}{5}}g^{-5/4}\chi^{-9/4}\exp\left(\frac{-g}{\chi v^2}\right) \tag{3}$$

Equation (3) gives the Pierson-Moskowitz sea surface wave spectrum, where A is the RMS power spectral density, χ is surface wavenumber and g is the acceleration due to gravity at the earth's surface. Different realisations of the sea surface are obtained by applying probability distributions to the amplitudes and phases of the spectrum. A zero mean normal distribution is applied to the amplitudes and the phases are uniformly distributed. Straightforward inverse Fast Fourier Transform (FFT) from wavenumber χ to range r gives the sea surface profile.

When Fourier methods are used for pulse propagation, stationarity of the ocean environment during the pulse travel time is assumed. This is a reasonable assumption owing to the slow changes in large scale oceanographic features, but could be questionable in the case of the sea surface. However, though the sea surface is likely to change to some extent over the pulse travel time, it may be considered stationary provided that two conditions are met. First, the movement must be slow compared to the pulse transmission duration; and second, that the ratio of acoustic wave speed to sea surface wave speed must be large so that Doppler effects are negligible. The first condition will generally be satisfied except for long pulses of the order of seconds in duration. The second condition depends upon the wind speed, as the sea surface wave propagation is governed by the dispersion relationship from which the phase speed is obtained as given below.

$$F = \sqrt{\frac{g}{2\pi\Lambda}} \tag{4}$$

The dispersion relationship is given in (4) in which F is the surface wave frequency and Λ is the surface wavelength, and the phase velocity is given by $U=F\Lambda$. The ratio of acoustic wave speed to sea surface wave speed depends upon sea state and is of the order of several hundred for surface waves of significant amplitude. Hence Doppler shifts of a few Hertz may occur. To a first approximation the surface can be considered stationary as the Doppler effects are small. However, by obtaining transfer functions for a series of temporal 'snapshots' of a time-varying ocean and using inverse FFTs to give a series of sequential filters, a time-dependent filter can be derived by simple linear interpolation between these snapshot filters. Doppler effects would appear naturally using this method, which could be used to model all variability of the ocean environment over the pulse travel time, e.g. sea surface movement and sound speed fluctuations in the water column. Hence, the frequency domain approach is not strictly limited to a stationary ocean environment. (Updating the ocean environment between pulses, i.e. modelling ping-to-ping variability, is achieved simply by computing a new transfer function for each ping).

3. Helmholtz integral method

For the case of an infinite isovelocity ocean and a single frequency pressure field, together with the Dirichlet (zero field) boundary condition, Thorsos [8,9] has proposed a benchmark model. The method used in this paper has been described in detail by Thorsos, and only a brief overview will be given here. The Thorsos model considers the two-dimensional scattering of a finite width beam by a rough surface. The Helmholtz integral formulation is used to derive a surface integral equation of the first kind.

$$p_i(\mathbf{r}) = \frac{1}{4i}\int_s H_0^{(1)}(k|\mathbf{r}-\mathbf{r}'|)\frac{\partial p(\mathbf{r}')}{\partial n'}ds' \tag{5}$$

In (5) the incident surface pressure field is $p_i(\mathbf{r})$, the total pressure field is $p(\mathbf{r}')$, vectors $\mathbf{r}$ and $\mathbf{r}'$ are on the rough surface defined by $y=h(x)$ where y is surface elevation as a function of horizontal distance x (range) and h is arbitrary, k is acoustic wavenumber and $H_0^{(1)}$ is the zeroth order Hankel function of the first kind. We use the differential operator $\frac{\partial}{\partial n'} = \hat{\mathbf{n}}.\nabla$, where $\hat{\mathbf{n}}$ is the outward normal unit vector to the rough surface and $ds' = (1+(dh(x')/dx')^2)^{1/2}$. The substitute variables for s and x are s' and x', where s is the position on the rough surface and x is the range.

In this adaptation of the method an incident field, defined at zero range as a function of depth (and also used as the PE starting field), is propagated to the rough surface to provide the incident surface pressure field, $p_i(\mathbf{r})$. This is used as input into the integral equation method. The solution of the surface integral equation provides the normal derivative of the total pressure field on the surface, $\frac{\partial p(\mathbf{r}')}{\partial n'}$. The scattered field is then computed as $p_{sc}(\mathbf{r}) = -\frac{1}{4i}\int_s H_0^{(1)}(k|\mathbf{r}-\mathbf{r}'|)\frac{\partial p(\mathbf{r}')}{\partial n'}ds'$. Finally the total acoustic field is obtained as the sum of the scattered and incident pressure fields, $p(\mathbf{r}) = p_i(\mathbf{r}) + p_{sc}(\mathbf{r})$.

The surface integral equation (5) is solved numerically by converting it into a matrix equation. This is achieved by discretisation of the surface into N range intervals of length $\Delta x=L/N$ where L is the total sea surface length being insonified. We typically have 10 or more intervals per acoustic wavelength. (As the ratio of acoustic wavelength to dominant sea surface wavelength is less than one for the frequency considered here (1500 Hz), the lower limit on the required number of intervals is determined by the acoustic wavelength). The starting field used is the Gaussian shaded plane wave beam defined below and is identical in form to that used by Thorsos.

$$\Psi(0,z) = \exp\left(\frac{-(z-z_s)^2}{\sigma^2}\right)\exp(ik\sin\theta_0 z) \tag{6}$$

$$\sigma = \frac{\sqrt{2\ln 2}}{k\sin\theta_1} \tag{7}$$

In (6) Ψ is the starting field (at range zero), z is depth, z_s is source depth, θ_0 is the source elevation angle and σ is defined in (7), in which θ_1 is the angle at which the magnitude response of the source is 3dB less than the response at 0°. The PE starting fields are required to vanish at the sea surface, and it was ensured that the fields defined by our test parameters have negligible magnitude at the surface.

4. Comparisons to reference solutions

The tests of the surface scattering method involve computing the pressure field as a function of depth for a frequency of 1500 Hz and a variety of source elevation angles and receiver ranges. The SPUR solutions are compared to the solutions from the Helmholtz integral method. In all cases, the source depth z_s=75 m and the 3 dB half-width angle θ_1=4°. The wind speed for typical sea surface generation is 10 ms^{-1}, and the water sound speed is 1500 ms^{-1}. Figures 1,2 and 3 show the pressure magnitudes as a function of depth for source elevation angles 30°, 45° and 60° at ranges 450 m, 300 m and 150 m respectively. The solid line is the Helmholtz integral solution and the dashed line the SPUR solution.

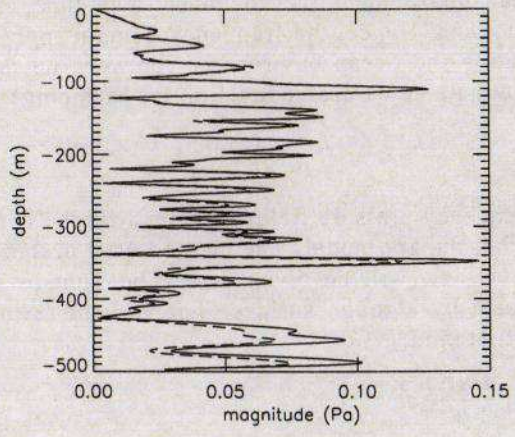

Figure 1. Source elevation angle 30°, range 450 m. Solid curve is the Helmholtz integral equation result, Dashed curve is the SPUR result.

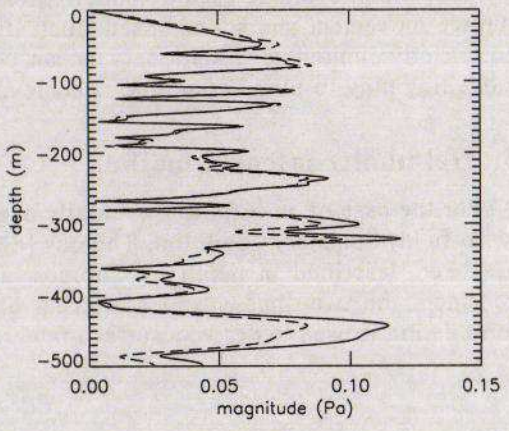

Figure 2. Source elevation angle 45°, range 300 m Solid curve is the Helmholtz integral equation result. Dashed curve is the SPUR result.

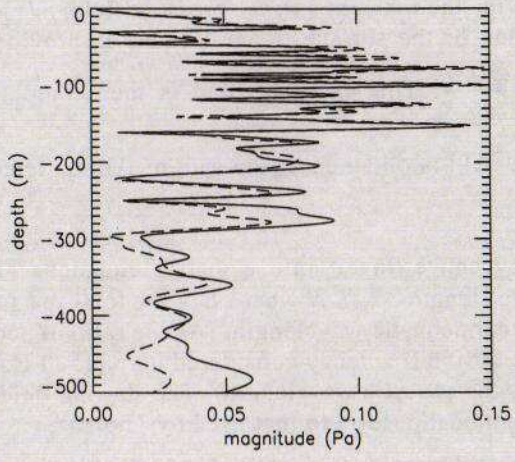

Figure 3. Source elevation angle 60°, range 150 m. Solid curve is the Helmholtz integral equation result. Dashed curve is the SPUR result.

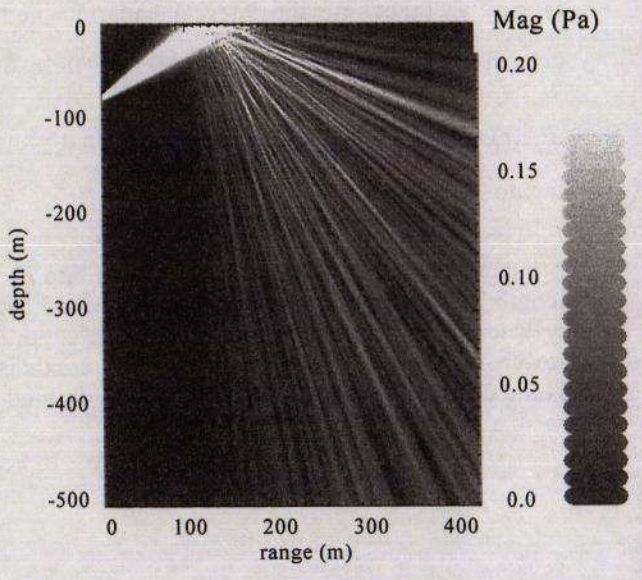

Figure 4. Source elevation angle 30°. Pressure field due to a finite beam incident upon a rough surface.

It is clear that agreement is close for shallow grazing angles but worsens for steep grazing angles. A nominal scattering angle of 45° corresponds to depths of 320 m, 225 m and 107 m in Figures 1, 2 and 3 respectively. It can be seen that the results are in close agreement up to and beyond this scattering angle range. For typical ocean acoustic propagation problems, sound travelling at angles above the seafloor critical angle will tend to be attenuated and have negligible contribution in the far field. As typical seafloor critical angles are seldom above about 30°, the surface scattering implementation can be used with confidence (Figure 1). In Figure 4, the pressure magnitude is plotted as a function of range and depth for the 30° source elevation angle (corresponding pressure at range 450 m shown in Figure 1). The dramatic re-distribution of energy with angle caused by the rough surface is clear.

5. Ocean environment

Studies have been made ([2], unpublished) of propagation from a point source in the upper layer of a bilinear sound speed profile (positive sound speed gradient down to a defined depth and negative gradient beyond to infinite depth). The bilinear profile is an idealised deep water profile. The surface scattering and surface loss implementations gave results differing by several dB over a range of 20 km. Here, comparisons of the surface loss and surface scattering methods are made for a shallow water environment with an absorbing seabed. There are two sound speed profiles (SSPs), representative of the summer and winter seasons. In Figure 5, the summer SSP consists of a surface duct overlying a thermocline below which is a deep duct. The winter SSP, shown in Figure 6, consists of a single duct. The water layer was given volume attenuation according to a standard formula [10]. The seabed is a homogeneous half space with a sound speed of 1700 ms^{-1}, a density of 1.5 gcm^{-3} and a volume attenuation coefficient of 0.5 dB/λ. The point source is at a depth of 50 m. The wind speed is 7 ms^{-1}.

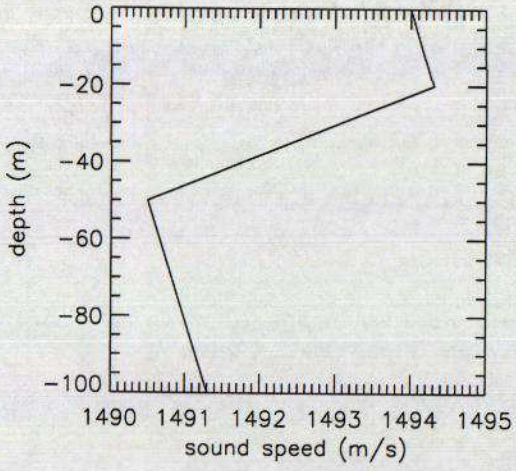

Figure 5. summer SSP

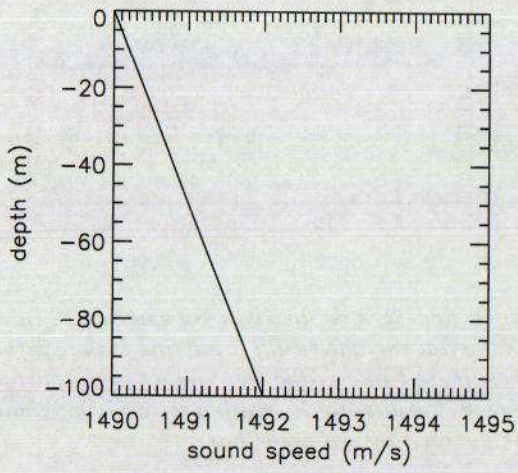

Figure 6. winter SSP

6. Results

Transmission loss (TL) as a function of range and depth at 1500 Hz is shown in Figure 7 for the summer SSP and Figure 8 for the winter SSP. In both cases a high degree of multipathing is apparent due to the reflective seabed. The results of Figures 7 and 8 were both generated with a rough surface (single realisation). For the summer SSP it is clear that beyond a range of about 15 km the dominant paths are those channelled between the deep duct and the thermocline. The net effect of the rough surface is to scatter surface-bottom bounce paths from sub- to super-critical angles and lose the energy to the absorbing seabed. In the case of the winter SSP all paths are surface-interacting and below the top 20 m of the water layer, TL is higher than for the summer SSP as no paths are channelled away from the surface.

We now examine the TL as a function of range at three receiver depths: 10 m (Figures 9 and 10), 35 m (Figures 11 and 12) and 75 m (Figures 13 and 14). For the summer SSP, Figures 9, 11 and 13 correspond to receiver depths at the centres of the surface duct, thermocline and deep duct respectively. For the winter SSP, Figures 10, 12 and 14 correspond to the same receiver depths for comparison.

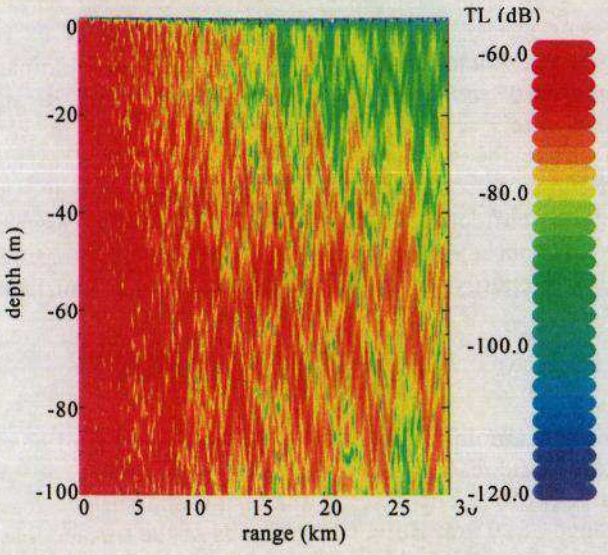

Figure 7. TL for summer SSP

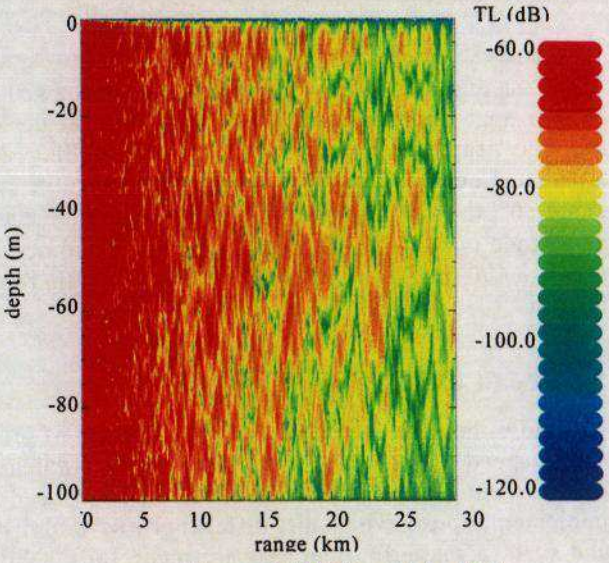

Figure 8. TL for winter SSP

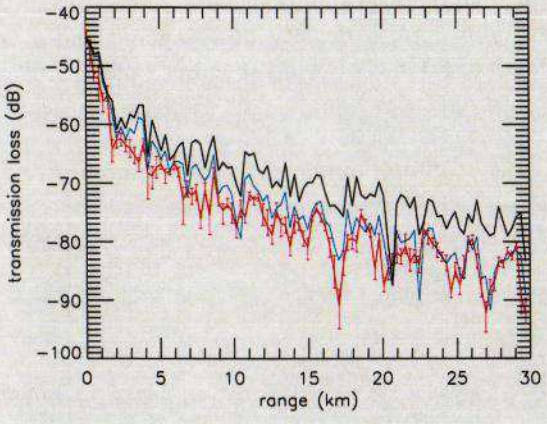

Figure 9. Receiver depth 10 m, summer SSP. Black line is the flat surface result, blue line is the surface loss result, red line is the average of eight surface scattering results with minimum and maximum values denoted by red error bars.

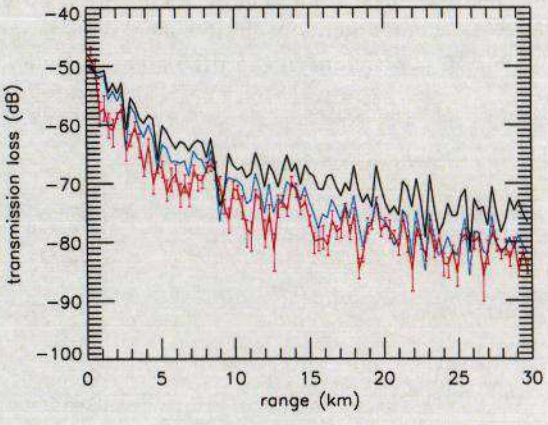

Figure 10. Receiver depth 10 m, winter SSP. Colour scheme is the same as Figure 9.

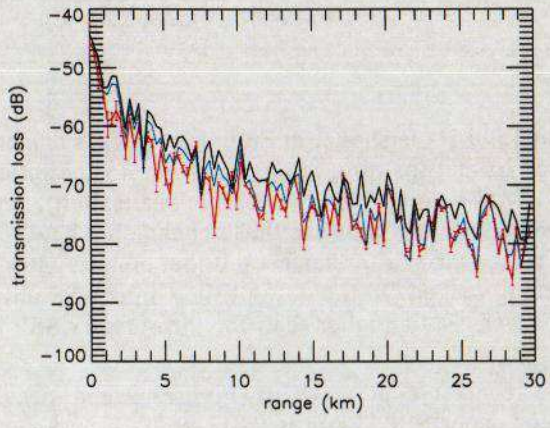

Figure 11. Receiver depth 35 m, summer SSP. Colour scheme is the same as in Figure 9.

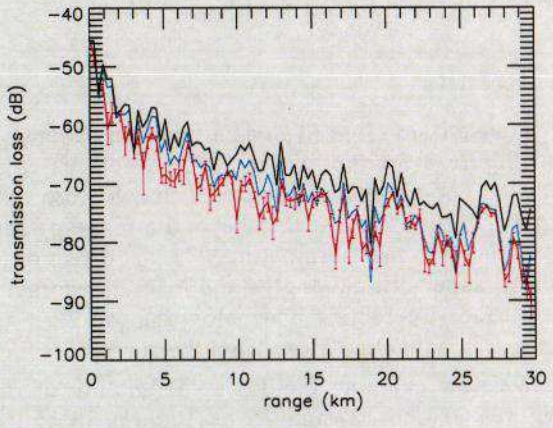

Figure 12. Receiver depth 35 m, winter SSP. Colour scheme is the same as in Figure 9.

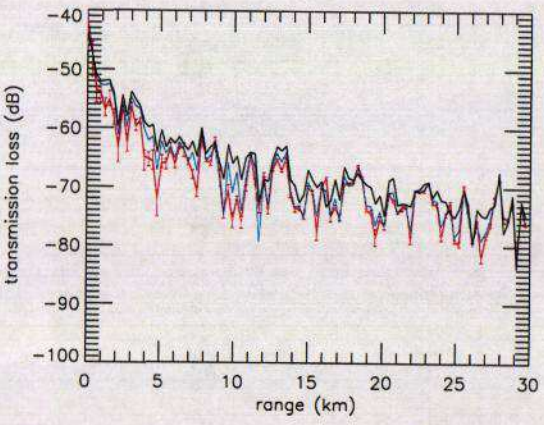

Figure 13. Receiver depth 75 m, summer SSP. Colour scheme is the same as in Figure 9.

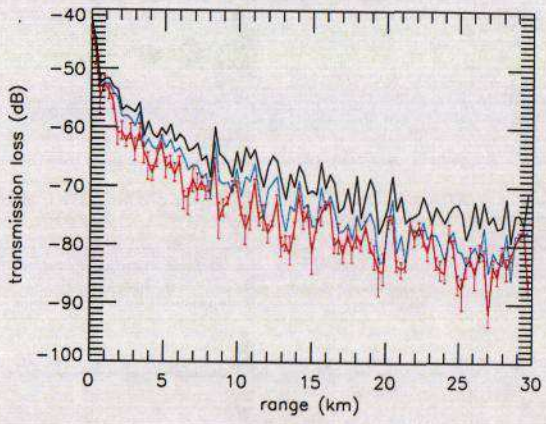

Figure 14. Receiver depth 75 m, winter SSP. Colour scheme is the same as in Figure 9.

In each figure the blue curve is the surface loss result, the red vertical lines at each range span the surface scattering results obtained from different surface realisations (eight realisations of the rough surface were generated and the results computed for each one), and the red curve is the average surface scattering result. The black curve is the flat surface (horizontal pressure-release boundary) result, included for reference and to illustrate the magnitude of the effect of the sea surface. The TL was computed every 100 m in range and the plots show results every 300 m: the result at each range is therefore an average of three values. The range-averaging was performed simply for clarity in the plots: results every 100m are too dense for clear interpretation on this range scale.

It is clear that the surface loss results predict lower losses than the surface scattering results. As range from the source increases, the surface interacting sound will be attenuated and contribute less to the total field, so we expect agreement between the loss and scattering results to improve with range, as seen in the results. Note that the spread of TL values from the multiple surface realisations is fairly constant with depth for the winter SSP, but decreases with increasing depth for the summer SSP. This is to be expected, as sound travelling at all depths is surface interacting with the winter SSP. In contrast, with the summer SSP, sound travelling below the surface duct has negligible interaction with the surface. As expected, the flat surface results are generally in error by a large margin: the sea surface clearly cannot be adequately represented by a horizontal pressure-release boundary at this frequency. The exception to this is for the summer SSP at receiver depths 35 m and 75 m: as sound travelling below the surface duct undergoes negligible surface interaction, representation of the surface is unimportant for these receiver depths, and all three curves are in quite close agreement.

We now transmit a 0.1s duration Hanning shaded sine wave pulse from the point source at depth 50 m to the three receivers (depths 10 m, 35 m and 75 m) at a range of 30 km. Figures 15 and 16 show the received pulses for the summer SSP with surface loss and surface scattering (single rough surface realisation) respectively. The differences between the surface loss and surface scattering results are apparent. At all receiver depths, the number of significant arrivals is lower with surface scattering than with surface loss. This is most apparent for the 10 m deep receiver, as sound travelling below the surface duct has negligible interaction with the surface. For the 35m and 75 m deep receivers, the scattering and loss results show greater similarity, but there are still noticeably more significant arrivals in the surface loss case. The surface scattering results contain some weak arrivals both before and after the main arrivals: these correspond to low amplitude scattered paths. As previously discussed, the net effect of the rough surface is to scatter surface-interacting sound from below to above the seabed critical angle, where it is attenuated and has negligible contribution in the far field. The surface loss method represents the gross effect of such processes as a simple reduction in the amplitude of the surface interacting paths. Both the TL results and the pulse results differ between the two surface representations: the pulse results allow particular insight into the differences between the surface loss and surface scattering methods.

7. Summary

Both surface loss and surface scattering methods have been implemented in a wide angle parabolic equation model. The surface scattering method has been verified by comparison to the Helmholtz integral method, with good agreement for the range of scattering angles relevant for practical ocean-acoustic propagation purposes.

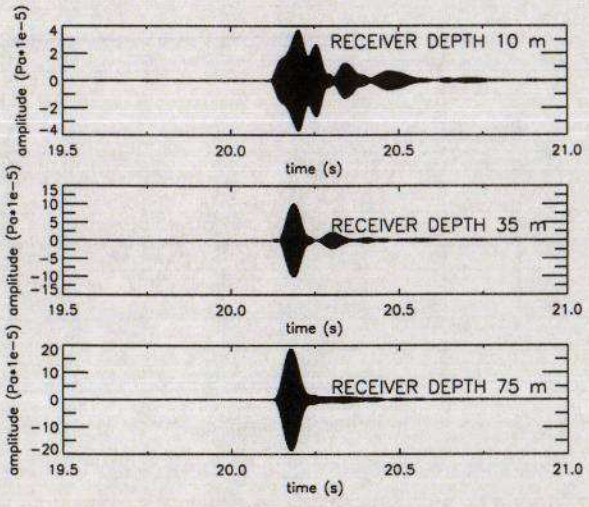

Figure 15. Received pulses with surface loss

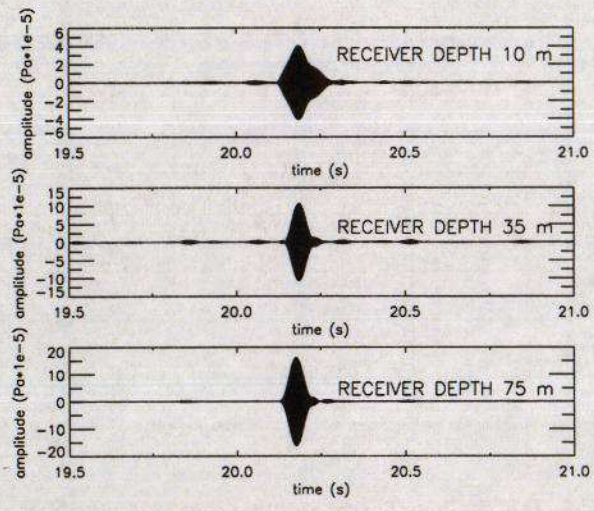

Figure 16. Received pulses with surface scattering

Propagation in a shallow water environment with a reflective seabed and both summer and winter sound speed profiles has been studied. Transmission loss at 1500 Hz showed the surface loss results to predict lower losses than the surface scattering results. Propagation of a 1500 Hz 0.1 s duration pulse to a range of 30 km showed differences in the arrival structures between the scattering and loss results. Differences between results from surface loss and surface scattering methods will of course be dependent upon the scenario (ocean environment, source and receiver depths, etc.). Investigation of different scenarios will help to determine those in which a surface loss formula method is an adequate representation of acoustic interaction with the sea surface.

References

[1] Holford RL. Scattering of sound waves at the ocean surface: A diffraction theory. *J. Acoust. Soc. Am.* 1981; **70**(4): 1103-1115.

[2] Donnelly MK, Hewitt RN, Clarke T and Prior MK. Pulse propagation by Fourier synthesis of wide angle parabolic equation solutions including forward scattering from a rough sea surface. Unpublished.

[3] Donnelly MK. Synthetic Pulse Reception (SPUR), in *Proceedings of the Undersea Defence Technology (Europe) 2000 Conference,* London, 2000.

[4] Collins MD. User's Guide for RAM Versions 1.0 and 1.0p. Naval Research Laboratory, Washington, DC 20375, 1995.

[5] Weston DE and Ching PA. Wind effects in shallow-water acoustic transmission. *J. Acoust. Soc. Am.* 1989; **86**(4): 1530-1545.

[6] Gilbert KE. Application of the parabolic equation to sound propagation in a refracting atmosphere. *J. Acoust. Soc. Am.* 1989; **85(2)**: 630-637.

[7] Pierson WJ Jnr and Moskowitz L. A proposed spectral form for fully developed wind seas based on the similarity theory of S.A Kitaigorodski. *Journal of Geophysical Research* 1964; **69**: 5181-5190.

[8] Thorsos EI. The validity of the Kirchoff approximation for rough surface scattering using a Gaussian roughness spectrum. *J. Acoust. Soc. Am.* 1988; **83**: 78-92.

[9] Thorsos EI. Test Case 1:Sea surface forward scattering, in *Benchmark Solutions in Reverberation and Scattering: Proceedings of the Reverberation and Scattering Workshop*, Naval Research Laboratory Book Contribution NRL/BE/7181-96-001, U.S Government Printing Office, Washington, DC, 1994, pp. 3.2-3.20.

[10] Jensen FB, Kuperman WA, Porter MB and Schmidt H. Computational Ocean Acoustics. AIP Press, New York, 1994, pp. 38.

This research was funded by the United Kingdom Ministry Of Defence Applied Research Programme.